Mon. Not. R. Astron. Soc. **000**, 1–6 (2000) Printed 1 February 2008 (MN LATEX style file v1.4)

On the second overtone stability among SMC Cepheids

G. Bono,[1,2] F. Caputo,[1] and M. Marconi,[3]
[1] *Osservatorio Astronomico di Roma, Via Frascati 33, 00040 Monte Porzio Catone, Italy*
[1] *Euroapen Southern Observatory, Casilla 19001, Santiago 19, Chile*
[3] *Osservatorio Astronomico di Capodimonte, Via Moiariello 16, 80131 Napoli, Italy*

1 February 2008

ABSTRACT

We present a new set of Cepheid, full amplitude, nonlinear, convective models which are pulsationally unstable in the second overtone (SO). Hydrodynamical models were constructed by adopting a chemical composition typical for Cepheids in the Small Magellanic Cloud (SMC) and stellar masses ranging from 3.25 to 4 $M_{\odot}$. Predicted ϕ_{21} Fourier parameters agree, within current uncertainties, with empirical data for pure first and second overtone variables as well as for first/second overtone (FO/SO) double-mode Cepheids collected by Udalski et al. (1999a,b) in the SMC. On the other hand, predicted I band amplitudes are systematically larger than the observed ones in the short period range, but attain values that are closer to the empirical ones for $\log P_{SO} \geq -0.12$ and $\log P_{FO} \geq 0.1$. We also find, in agreement with empirical evidence, that the region within which both second and first overtones attain a stable limit cycle widens when moving toward lower luminosities. Moreover, predicted P_{SO}/P_{FO} and P_{FO}/P_F period ratios agree quite well with empirical period ratios for FO/SO and F/FO double-mode SMC Cepheids.

Interestingly enough, current models support the evidence that pure SO Cepheids and SO components in FO/SO Cepheids are good distance indicators. In fact, we find that the fit of the predicted Period-Luminosity-Color (V, V-I) relation to empirical SMC data supplies a distance modulus of 19.11 ± 0.08 mag. The same outcome applies to pure FO Cepheids and FO components in FO/SO Cepheids, and indeed we find DM=19.16 ± 0.19 mag. Current distance estimates do not account for, within current uncertainties on photometry and reddening, the so-called short distance scale.

Key words: Cepheids — Magellanic Clouds — stars: distances — stars: oscillations.

1 INTRODUCTION

The existence of overtone pulsators among radial variables is a long-standing astrophysical problem (Eddington 1926; Ledoux & Walraven 1958). On the basis of pulsating polytropic models, Schwarzschild (1941) suggested that among actual RR Lyrae variables are present both fundamental -$RR_{\rm ab}$- and first overtone -$RR_{\rm c}$- pulsators. This identification was facilitated by the empirical evidence that the pulsation amplitude and shape of the light curve of the two groups are quite different. The same outcome does not apply to high amplitude δ Scuti stars (McNamara 2000) and classical Cepheids, since fundamental (F) and overtone pulsators do show quite similar light curves nor the pulsation amplitudes can be safely adopted to identify the pulsation mode (Santolamazza et al. 2000).

The occurrence of FO pulsators among classical Cepheids was originally suggested by Pel & Lub (1978), but their existence was a matter of concern till few years ago (Bohm-Vitense 1994) and it was definitively settled by the large sample of variable stars collected by the microlensing experiments (MACHO, EROS, OGLE). These teams also reported the detection of some tens of double-mode Magellanic Cepheids pulsating simultaneously in the first and in the second overtone (Beaulieu et al. 1997; Alcock et al. 1999; Udalski et al. 1999a, U99a). Even though, the existence of pure SO Cepheids was originally predicted by Stobie (1969) only two candidates (Galaxy, Burki et al. 1986; LMC, Alcock et al. 1999) have been proposed. Useful hints on the selection criteria to single out SOs were suggested by Antonello & Kanbur (1997, AK97) on the basis of nonlinear SO models. However, the existence and the observational properties of these objects were rooted to the ground by Udalski et al. (1999b, U99b) who found a dozen low-amplitude, short-period SOs in a sample of 2300 SMC Cepheids.

The main aim of this investigation is to present Cepheid full amplitude, convective SO models and compare theoretical predictions with observed SO Cepheids in the SMC. We

selected these variables because we are interested in testing whether nonlinear, convective models account for the pulsation behavior of relatively metal-poor Cepheids. In fact, it has been recently suggested that current turbulent convective (TC) models do not account for energy dissipation sources in metal-poor Cepheids (Feuchtinger et al. 2000). At the same time, we are also interested in assessing whether SOs can be safely adopted to estimate stellar distances. Finally, we also computed nonlinear FO models, to figure out how the instability strip changes when moving toward lower luminosities.

2 THEORETICAL MODELS AND DATA

The full amplitude, nonlinear convective models presented in this investigation were constructed by adopting the input physics and physical assumptions discussed in Bono, Caputo, & Marconi (1998, BCM) and in Bono, Marconi & Stellingwerf (1999, BMS). In contrast with BCM and BMS we assumed a vanishing efficiency of turbulent overshooting in the regions where the superadiabatic gradient attains negative values. In fact, nonlinear, convective RR Lyrae models constructed by adopting this assumption account for the luminosity variation over a full cycle of U Com a field RR_c variable (Bono, Castellani, & Marconi 2000). Numerical experiments performed by adopting the same input parameters adopted by BMS suggest that the stability and the shape of the light curve of F Cepheid models are marginally affected by this assumption. However, the luminosity amplitudes of both first and second overtones roughly decrease by 24%.

To cover the observed period range of SO Cepheids we constructed four different sequences of models at fixed chemical composition Y=0.25, Z=0.004 and stellar masses equal to 3.25, 3.5, 3.8, and 4.0 $M_{\odot}$. The luminosity of these models was fixed according to the mass-luminosity (ML) relation adopted by BCM and BMS. Recent calculations (Bono et al. 2000) based on up-to-date canonical evolutionary models which cover a wide range of He and metal contents support this choice. To assess how the topology of the instability strip changes when moving toward lower luminosities, the previous models were implemented with three series of FOs with stellar masses equal to 5.0, 5.5, and 5.8 $M_{\odot}$. The static models were forced out of equilibrium by imposing a velocity amplitude of $5 km s^{-1}$ to the radial eigenfunctions. The nonlinear equations are integrated in time until the pulsation amplitudes show, over consecutive cycles, a periodic similarity of the order of 10^{-4}.

Table 1 summarizes the input parameters and selected nonlinear observables for the sequences of first and second overtone models. From left to right the first three columns give the stellar mass, the luminosity and the effective temperature (K), while columns (4) to (6) list the period (d), the mean radius, and the fractional radius. Columns (7) to (9) give the bolometric (mag), the radial velocity (Km/s), and the effective temperature (K) amplitudes, while the last three columns list the I band amplitudes, as well as the Fourier parameters ϕ_{21} and R_{21}.

Fig. 1 shows the run of bolometric light and radial velocity curves over two consecutive cycles. Data plotted in this figure show two interesting features: i) both luminosity and velocity curves do show, in agreement with empirical evidence, smooth changes over the full pulsation cycle. However, few light curves show a small bump along the rising branch. It is not clear, whether this is a drawback of theoretical models, since one of the criteria adopted to select pure SO pulsators is a sinusoidal luminosity variation along the pulsation cycle. Note that the 9 pure SO pulsators we selected (see below) according to the Wesenheit index present light curves that are somewhat noisy, and therefore the bump can be barely detected. ii) SO luminosity, radius, and velocity amplitudes are approximately a factor of two smaller than FO amplitudes. On the other hand, the temperature amplitudes are roughly a factor of three smaller (see column (9) in Table 1). This suggests that the SO luminosity changes are mainly governed by radius rather than by temperature variations. Note that current SO bolometric and radial velocity amplitudes appear to be smaller than predicted by AK97. However, AK97 adopted a slightly different He and metal contents (Y=0.29, Z=0.01 against Y=0.25, Z=0.004).

Figure 1. Bolometric light curves (left) and radial velocity curves (right) along a full pulsation cycle versus phase. The curves refer to models constructed by adopting different masses (see labeled values). The nonlinear periods (d), and the effective temperatures (K) are listed in the left and in the right panel respectively.

We first consider the modal stability of the selected Cepheid models. In order to compare theory and observations the predicted instability edges were transformed into the observational plane by adopting the bolometric corrections and color-temperature relations derived by Castelli, Gratton, & Kurucz (1997). Fig. 2 shows the topology of the Cepheid instability strip for the first three radial modes in the $M_V, V-I$ Color Magnitude (CM) diagram.

A glance at the data plotted in this figure shows that the region within which the SO is unstable widens when moving from high to low luminosities, and indeed the temperature width increases from 100 K to almost 500 K. The same outcome applies to the OR region, i.e. the region in which both SO and FO pulsators are unstable, and indeed its temperature width for M=3.25 $M_{\odot}$ is roughly equal to 200 K. Moreover, predicted period ratios -P_{SO}/P_{FO}- in this region range from 0.799 to 0.805 and are in fair agreement with empirical values ($0.802 \div 0.809$, U99a). The widening

Table 1. Input parameters and selected nonlinear second and first overtone observables (Y=0.25, Z=0.004).

M[1]	$\log L$[1]	T_e K	Period d	R[1]	$\Delta R/R$	ΔM_{bol} mag	Δu Km/s	ΔT_e K	A_I mag	Φ_{21}	R_{21}
					Second Overtone						
3.25	2.49	6850	0.5037	12.496	0.020	0.362	25.60	600	0.248	4.173	0.224
3.25	2.49	6800	0.5177	12.724	0.029	0.500	37.34	850	0.342	4.201	0.298
3.25	2.49	6700	0.5406	13.155	0.035	0.516	44.21	950	0.400	4.246	0.337
3.25	2.49	6600	0.5664	13.536	0.039	0.482	51.34	750	0.345	4.358	0.302
3.25	2.49	6500	0.5942	13.904	0.039	0.385	49.98	600	0.288	4.633	0.248
3.50	2.61	6750	0.6319	14.869	0.019	0.307	22.78	500	0.215	4.249	0.196
3.50	2.61	6700	0.6437	15.107	0.029	0.424	33.32	700	0.291	4.283	0.252
3.50	2.61	6600	0.6747	15.495	0.038	0.480	44.15	750	0.333	4.352	0.278
3.50	2.61	6500	0.7067	16.013	0.039	0.409	44.93	600	0.298	4.632	0.216
3.80	2.74	6700	0.7826	17.415	0.001	0.015	1.08	50	0.011	4.592	0.105
3.80	2.74	6600	0.8105	18.004	0.023	0.333	26.25	550	0.247	4.438	0.173
4.00	2.82	6600	0.9140	19.678	0.005	0.074	5.34	100	0.052	4.789	0.028
					First Overtone						
3.25	2.49	6600	0.7049	13.573	0.077	1.099	83.56	1850	0.731	4.001	0.379
3.25	2.49	6500	0.7377	14.041	0.082	0.975	86.65	1600	0.670	4.037	0.344
3.25	2.49	6100	0.9015	15.811	0.066	0.365	57.16	700	0.268	4.765	0.281
3.50	2.61	6600	0.8381	15.599	0.075	1.114	79.09	1900	0.721	3.971	0.420
3.50	2.61	6500	0.8848	16.060	0.081	1.026	81.78	1850	0.656	3.972	0.410
3.50	2.61	6400	0.9285	16.656	0.084	0.873	81.18	1850	0.594	3.979	0.389
3.50	2.61	6200	1.0256	17.673	0.081	0.536	71.90	1650	0.397	4.225	0.320
3.50	2.61	6100	1.0805	18.167	0.074	0.440	62.65	1550	0.324	4.657	0.336
3.50	2.61	6000	1.1331	18.705	0.060	0.338	49.06	600	0.248	4.870	0.401
3.80	2.74	6600	1.0150	18.105	0.117	0.956	56.30	1600	0.635	4.004	0.423
3.80	2.74	6400	1.1179	19.202	0.071	0.857	68.65	1150	0.673	4.102	0.487
3.80	2.74	6300	1.1775	19.918	0.151	0.798	70.22	1500	0.568	4.211	0.474
3.80	2.74	6200	1.2375	20.545	0.069	0.549	62.81	850	0.445	4.434	0.418
3.80	2.74	6000	1.3720	21.765	0.060	0.440	47.96	600	0.276	4.989	0.408
4.00	2.82	6600	1.1403	19.787	0.023	0.351	19.71	550	0.248	4.016	0.230
4.00	2.82	6000	1.5483	23.963	0.063	0.392	50.81	650	0.296	5.077	0.362
4.00	2.82	5900	1.6221	24.687	0.050	0.291	38.10	500	0.224	5.058	0.434
5.00	3.07	6400	1.7495	28.033	0.059	0.830	47.61	1300	0.583	4.236	0.437
5.00	3.07	6200	1.9425	29.977	0.067	0.811	64.62	1200	0.601	4.444	0.456
5.00	3.07	5900	2.2800	32.969	0.062	0.374	49.08	600	0.296	5.259	0.338
5.50	3.32	6400	2.6553	37.230	0.002	0.022	1.15	50	0.016	5.036	0.445
5.50	3.32	6200	2.9179	39.858	0.049	0.553	36.03	850	0.411	6.013	0.094
5.50	3.32	6000	3.2626	42.494	0.060	0.512	45.58	750	0.402	4.588	0.310
5.80	3.40	6400	2.9627	40.931	0.001	0.014	0.86	50	0.011	5.124	0.208
5.80	3.40	6200	3.2911	43.599	0.011	0.132	7.44	200	0.098	5.471	0.235
5.80	3.40	6000	3.6780	46.756	0.060	0.505	41.53	700	0.401	4.739	0.077

[1] Stellar masses, luminosities and radii are in solar units.

of the SO instability strip is mainly caused by the fact that the decrease in luminosity causes a substantial decrease in the SO total kinetic energy when compared with the FO. In fact, along the FOBE the ratio between SO and FO kinetic energy ranges from 0.66 at $M/M_\odot$=5 to 0.55 at $M/M_\odot$=4, and to 0.39 at $M/M_\odot$=3.25. A decrease in the SO total kinetic energy implies a decrease in the pulsation inertia of the envelope, and in turn in the amount of energy necessary to destabilize this mode (Gilliland et al. 1998).

Data plotted in Fig. 2 also show that the width of the FO instability region remains almost constant when moving from 5 to 3.25 $M_\odot$, whereas the width of the F region decreases from 400 K to 200 K. The narrowing of the F region is mainly due to a sharp change in the slope of the red edge at lower luminosities. This finding supports the empirical evidence recently brought out by Bauer et al. (1999) that when moving toward lower luminosities the number of F pulsators decreases and the slope of the PL relation for this mode changes. A more quantitative analysis of this effect will be addressed in a forthcoming paper (Bono et al. 2000). We also note that, the width of the OR region between F and FO remains constant and for $M \leq 3.8 M_\odot$ it becomes a factor of two smaller than the OR region between FO and SO. This difference supplies a qualitative explanation to the empirical evidence that among double-mode SMC Cepheids the 25% are F/FO, while the other are FO/SO variables (U99a). We also find that, the predicted period ratios P_{FO}/P_F in this region range from 0.725 to 0.746 that are once again in very good agreement with the observed ones ($0.728 \div 0.746$, U99a). Moreover, it is worth underlining that the total width of the instability strip, in the above mass range, remains constant and roughly equal to 1000 K. This means that when accounting for F, FO, and SO variables the edges of the Cepheid instability strip in the SMC are approximately parallel. It goes without saying that the occurrence of two OR regions makes fainter SMC Cepheids

Figure 2. Topology of the Cepheid instability strip for the first three radial modes in the CM diagram. Solid and dashed lines refer to blue and red edges respectively. The arrows mark the OR regions between first and second overtone (FO/SO) as well as between fundamental and first overtone (F/FO).

Figure 4. Comparison between predicted and observed amplitudes (top) and ϕ_{21} Fourier parameters (bottom). Amplitudes and ϕ_{21} values refer to the I band light curves. Theoretical and empirical curves were fitted with Fourier series which include 8 terms. The symbols are the same as in Fig. 3.

Figure 3. Wesenheit index vs period for pure SO pulsators (open circles, U99b), SO component in FO/SO Cepheids (open squares, U99a), pure FO pulsators (filled circles, U99b), FO component in FO/SO Cepheids (filled squares, U99a). Open triangles show the new selected SO pulsators, while solid and dashed lines display the predicted Wesenheit indices for second and first overtones respectively. Data were plotted by assuming DM=19.1 mag.

key objects to constrain predictions on the topology of the instability strip and on modal selection (Kollath 1999).

To properly identify pure SO pulsators in SMC, U99b adopted three different selection criteria, namely the Fourier parameters together with the location in both the Color-Magnitude and the PL diagram. The range of plausible R_{21} and ϕ_{21} values was selected, according to Alcock et al. (1999), on the basis of Fourier parameters of SO light curves in double-mode pulsators, while the period range was selected according to the P_{SO}/P_{FO} period ratio. By using these criteria U99b found 13 bona fide pure SO pulsators. We can now check whether the selection criteria they adopted are supported by current nonlinear convective models. Fig. 3 shows the comparison between the Wesenheit index of pure SO pulsators detected by U99b and predicted SO models (solid line). Although few objects seem to be systematically brighter/cooler than predicted the agreement between theory and observations is quite satisfactory.

Note that current predictions suggest that some FO variables which do not obey to the selection criteria adopted by U99b could be pure SO pulsators, since they are located in the same region covered by theoretical models. As a preliminary but plausible assumption we decided to include in the sample of pure SO pulsators the FO variables located within three σ (σ_W=0.03 mag, Udalski 2000, private communication) from the predicted SO loci. Interestingly, enough we find that the color distribution of the new candidates (open triangles) are quite similar to the V-I colors of FO/SO Cepheids, and indeed they range from 0.45 to 0.65 (U99a). Finally, we also included in Fig. 3 the FO/SO double-mode Cepheids to test whether current models do account for their distribution. The adopted periods, mean magnitudes and colors refer to data given by U99a (see their Appendix C). The physical assumptions adopted for constructing current nonlinear, convective models are somehow supported by the agreement between theory and observations. However, before any firm conclusion on the TC model currently adopted can be reached predictions based on nonlinear convective models should account for the entire observational scenario, and in particular for mixed-mode variables, and Fourier coefficients of F and FO Cepheids (Feuchtinger et al. 2000).

Fig. 4 shows the comparison between predicted and observed luminosity amplitudes (top panel) as well as ϕ_{21} (bottom panel) values. Data plotted in this figure refer to the Fourier fit of the I band light curves of SO components in FO/SO Cepheids and to pure SO Cepheids. Predicted amplitudes (filled triangles) up to $\log P \approx -0.15$ are systematically larger than the observed ones, whereas at longer periods they are quite similar to empirical ones.

Theoretical ϕ_{21} values are, within current uncertainties, in fair agreement with observed data for pure SO variables. The same outcome applies for the bulk of the ϕ_{21} values of the SO components in FO/SO Cepheids. The error bars for these objects are larger because the SO is the secondary mode and therefore their luminosity amplitudes are relatively small. Predicted and empirical R_{21} parameters are also in plausible agreement but unfortunately the latter

Figure 5. Same as Fig. 4 but for FO pulsators.

Figure 6. Period-Luminosity-Color (V,V-I) relations for second (top) and first (bottom) overtone pulsators. Solid lines show theoretical relations, while the symbols are the same as in Fig. 3.

ones are affected by large errors. Data plotted in the top panel support the evidence that the luminosity amplitudes can be safely adopted for selecting pure SO pulsators, since in this period range they are systematically smaller than FO amplitudes (Fig. 5). At the same time, the selection criterium based on the Fourier parameters of SO components in FO/SO Cepheids does not seem appropriate, since the SOs cover the same region covered by FOs (Figs. 4 and 5).

Fig. 5 shows the same data of Fig. 4 but they refer to pure FOs and to FO components in FO/SO Cepheids. Once again predicted amplitudes are, at short periods, systematically larger than the observed ones, whereas for periods longer than $\log P \approx 0$ the theoretical amplitudes attain values closer to the empirical ones. On the other hand, predicted ϕ_{21} values agree quite well with observations for periods shorter than $\log P = 0.4$. Note that theoretical models for $M/M_{\odot}$=5.5 and 5.8 show for $0.4 < \log P \leq 0.5$ a well-defined minimum in the pulsation amplitude, whereas predicted ϕ_{21} values are, in the same period range, larger than the empirical ones. More detailed calculations are necessary to assess whether this feature is connected with the occurrence of a Hertzsprung progression among FOs (Kienzle et al. 1999).

To disclose whether SOs are good standard candles we derived on the basis of current SO models the following analytical Period-Luminosity-Color (PLC) relation:

$$\begin{array}{llll} M_V = & 3.961 & -3.905 \log P & +3.250(V-I) \\ & \pm 0.005 & \pm 0.019 & \pm 0.054 \end{array}$$

where M_V and (V-I) are weighted mean intensities transformed into magnitudes, P is the period (d), and the standard deviation is 0.004. The spread of this relation is small because the temperature width of SO instability strip is substantially smaller than F and FO strips.

The top panel of Fig. 6 shows the projection of the PLC relation into a plane. Interestingly enough, we find that by fitting the sample of pure SO pulsators together with the FO/SO Cepheids the SMC distance modulus is 19.11 ± 0.08 mag. The uncertainty accounts for errors on both photometry and reddening but does not account for depth effects. Owing to the lack of individual reddening estimates we adopted, according to Caldwell & Coulson (1986), a mean reddening value of $E(B-V) = 0.054 \pm 0.029$. The current SMC distance estimate supports the distance determination derived by Bono et al. (1999, $DM = 19.19 \pm 0.17$ mag) on the basis of the fundamental PLC (V, B-V) relation and data available in the literature. Our distance estimate is in very good agreement with the SMC distance derived by Laney & Stobie (1994) on the basis of empirical PL relations in four different photometric bands i.e. $DM = 18.94 \pm 0.04$ mag (internal error), by Kovacs (2000) using double-mode SMC Cepheids ($DM = 19.05 \pm 0.13$ mag), and by Groenewegen (2000) using both the Wesenheit index ($DM = 19.08 \pm 0.11$ mag) and the PL_K relation ($DM = 19.04 \pm 0.17$ mag).

Forced by the above result we decided to estimate the SMC distance by adopting the theoretical PLC relation for FOs. By taking into account current and old (Bono et al. 1999) models we find the following PLC (V, V-I) relation: $M_V = 3.61(\pm 0.03) - 3.85(0.02) \log P + 3.33(\pm 0.09)(V-I)$ where the symbols have their usual meaning and the standard deviation is 0.03. The fit of this relation to both pure FOs and FO/SO Cepheids (see bottom panel of Fig. 6) supplies $DM = 19.16 \pm 0.19$ mag. The mean magnitudes and colors of these variables were corrected by adopting the same mean reddening adopted for SO variables. Even though FOs cover different period and luminosity ranges, the new distance agrees, within the errors, with the distance based on SOs. At the same time, both of them are at odds with SMC distances based on red clump stars ($DM = 18.63 \pm 0.07$ mag) and on field RR Lyrae stars ($DM = 18.66 \pm 0.16$ mag) derived by Udalski (1998) and by Udalski et al. (1998). Finally, we note that FO models for $M/M_{\odot}$=5 allow us to test the dependence of predicted FO edges on the adopted TC calibration. Interestingly enough, the new edges differ by less than 100 K when compared with the edges predicted by Bono et al. (1999) on the basis of the old TC calibration (Bono & Stellingwerf 1994). Therefore, it turns out that the new TC calibration marginally affects predicted PL and PLC relations.

3 CONCLUSIONS

We have presented and discussed theoretical predictions concerning the pulsation properties of SO pulsators among SMC Cepheids. The comparison between theory and observations brought out the following results: i) current metal-poor, nonlinear, convective models account for the pulsation behavior of pure first and second overtone Cepheids. In fact, predicted ϕ_{21} parameters are in fair agreement with empirical data (U99a,U99b). ii) Theoretical predictions show that the OR region, i.e. the region in which both first and second overtones are unstable, widens in temperature when moving from higher to lower luminosities. This evidence supplies a qualitative explanation to the large number of FO/SO double-mode Cepheids detected by OGLE in the SMC. iii) Predicted period ratios -P_{SO}/P_{FO}, P_{FO}/P_F- of the models located in the two OR regions are in good agreement with observed values for FO/SO and F/FO double-mode SMC Cepheids (U99a).

Interestingly enough we find that both pure SO variables and the SO components in FO/SO Cepheids are good distance indicators, and indeed the fit of the theoretical PLC (V,V-I) relation to empirical SMC data supplies a distance modulus of 19.11 ± 0.08 mag. This result is further strengthened by the fact that the distance modulus we obtain by adopting the predicted PLC relation for FO variables is 19.16 ± 0.19 mag. These distance estimates are based on a mean reddening correction, since the SMC Cepheid sample collected by OGLE lack of individual reddening measurements. Current distance estimates are, within the uncertainties, at odds with the so-called short distance scale.

ACKNOWLEDGMENTS

We thank V. Castellani for a critical reading of an early draft of this manuscript and D. Laney for useful discussions on reddening estimates. We also acknowledge A. Udalski for many helpful advice to retrieve data from the OGLE database, M. Groenewegen for communicating his results in advance of publication, and an anonymous referee for useful comments that improved the content of this paper. This work was supported by MURST -Cofin98- under the project: "Stellar Evolution".

REFERENCES

Alcock C. et al., 1999, AJ, 117, 920
Antonello E., Kanbur S. M., 1997, MNRAS, 286, 33 (AK97)
Bauer F., et al. 1999, A&A, 348, 175
Beaulieu J. P. et al., 1997, A&A, 318, L47
Bohm-Vitense E., 1994, AJ, 107, 673
Bono G., Caputo F., Cassisi S., Marconi M., Piersanti L., Tornambè A., 2000, ApJ, accepted, astro-ph/0006251
Bono G., Caputo F., Castellani V., Marconi M. 1999, ApJ, 512, 711
Bono G., Caputo F., Marconi M., 1998, ApJ, 497, L43 (BCM)
Bono G., Castellani V., Marconi M., 2000, ApJ, 532, L129
Bono G., Marconi M., Stellingwerf R. F. 1999, ApJS, 122, 167 (BMS)
Bono G., Stellingwerf R. F. 1994, ApJS, 93, 233
Burki G. et al., 1986, A&A, 168, 139
Caldwell J. A. R., Coulson I. M. 1986, MNRAS, 218, 223
Castelli F., Gratton R. G., Kurucz R. L. 1997, A&A, 324, 432
Eddington A. S., 1926 in The Internal Constitution of the Stars, Cambridge University Press, Cambridge, p. 203
Feuchtinger M. U., Buchler J. R., Kollath Z., 2000, ApJ, submitted, astro-ph/0005230
Gilliland R. L., Bono G., Edmonds P. D., Caputo F., Cassisi S., Petro L. D., Saha A., Shara M. M., 1998, ApJ, 507, 818
Groenewegen M. A. T. 2000, A&A, accepted, astro-ph/0010298
Kienzle F., Moskalik P., Bersier D., Pont F. 1999, A&A, 341,818
Kollath Z. 2000, in IAU Coll. 176, The Impact of Large-Scale Surveys on Pulsating Star Research, eds. Szabados, L. Kurtz, D., ASP, San Francisco, p. 356
Kovacs G. 2000, A&A, 360, L1
Laney C. D., & Stobie R. S. 1994, MNRAS, 266, 441
Ledoux P., & Walraven Th. 1958, in Handbuch der Physik, 51, 353
McNamara D. H. 2000, PASP, 112, 1096
Pel J. W., Lub J., 1978 in The HR diagram - The 100th anniversary of H. N. Russell, Reidel, Dordrecht, p. 229
Santolamazza P. Marconi M., Bono G., Caputo F., Cassisi S., & Gilliland R. L. 2000, ApJ, submitted
Schwarzschild M., 1941, ApJ, 94, 245
Stobie R. S., 1969, MNRAS, 144, 511
Udalski A., 1998, AcA, 48, 113
Udalski A., Pietrzynski G.; Wozniak P., Szymanski M., Kubiak, M., Zebrun , K 1998, ApJ, 509, L25
Udalski A. et al., 1999a, AcA, 49, 1 (U99a)
Udalski A. et al., 1999b, AcA, 49, 45 (U99b)

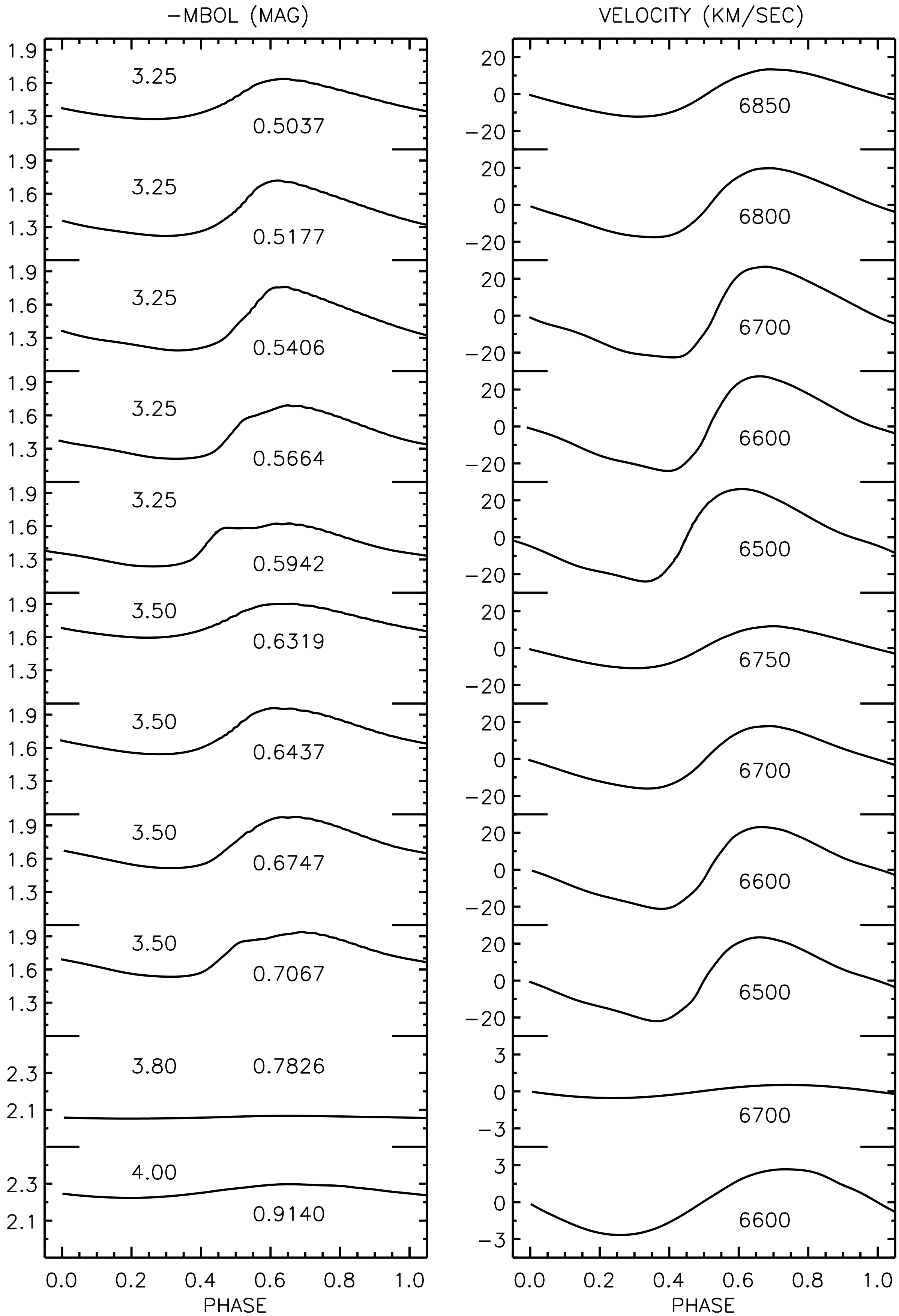

−MBOL (MAG)
VELOCITY (KM/SEC)
3.25
0.5037
6850
3.25
0.5177
6800
3.25
0.5406
6700
3.25
0.5664
6600
3.25
0.5942
6500
3.50
0.6319
6750
3.50
0.6437
6700
3.50
0.6747
6600
3.50
0.7067
6500
3.80
0.7826
6700
4.00
0.9140
6600
PHASE
PHASE

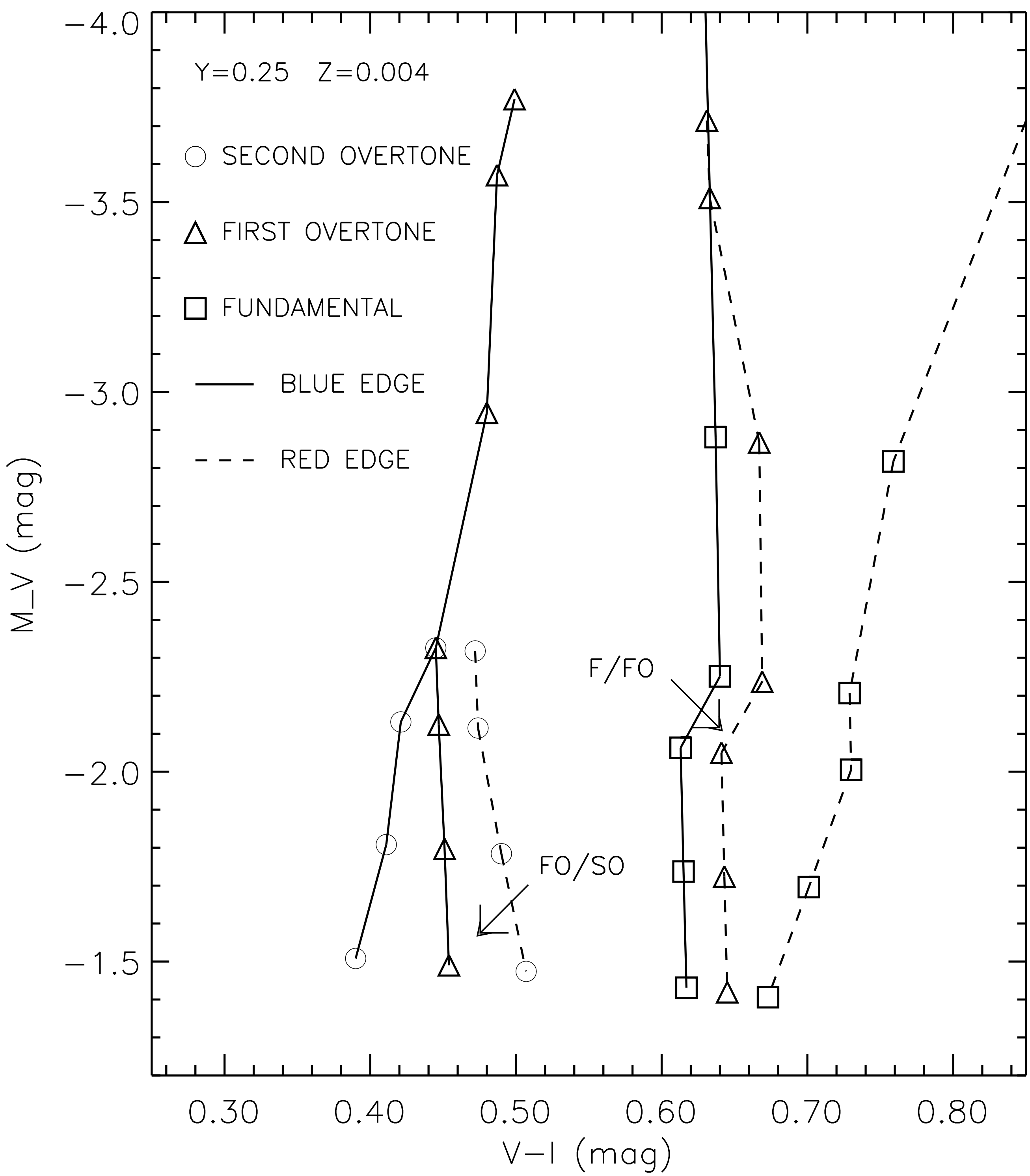

Y=0.25 Z=0.004
SECOND OVERTONE
FIRST OVERTONE
FUNDAMENTAL
BLUE EDGE
RED EDGE
F/FO
FO/SO
M_V (mag)
V−I (mag)
−4.0
−3.5
−3.0
−2.5
−2.0
−1.5
0.30
0.40
0.50
0.60
0.70
0.80

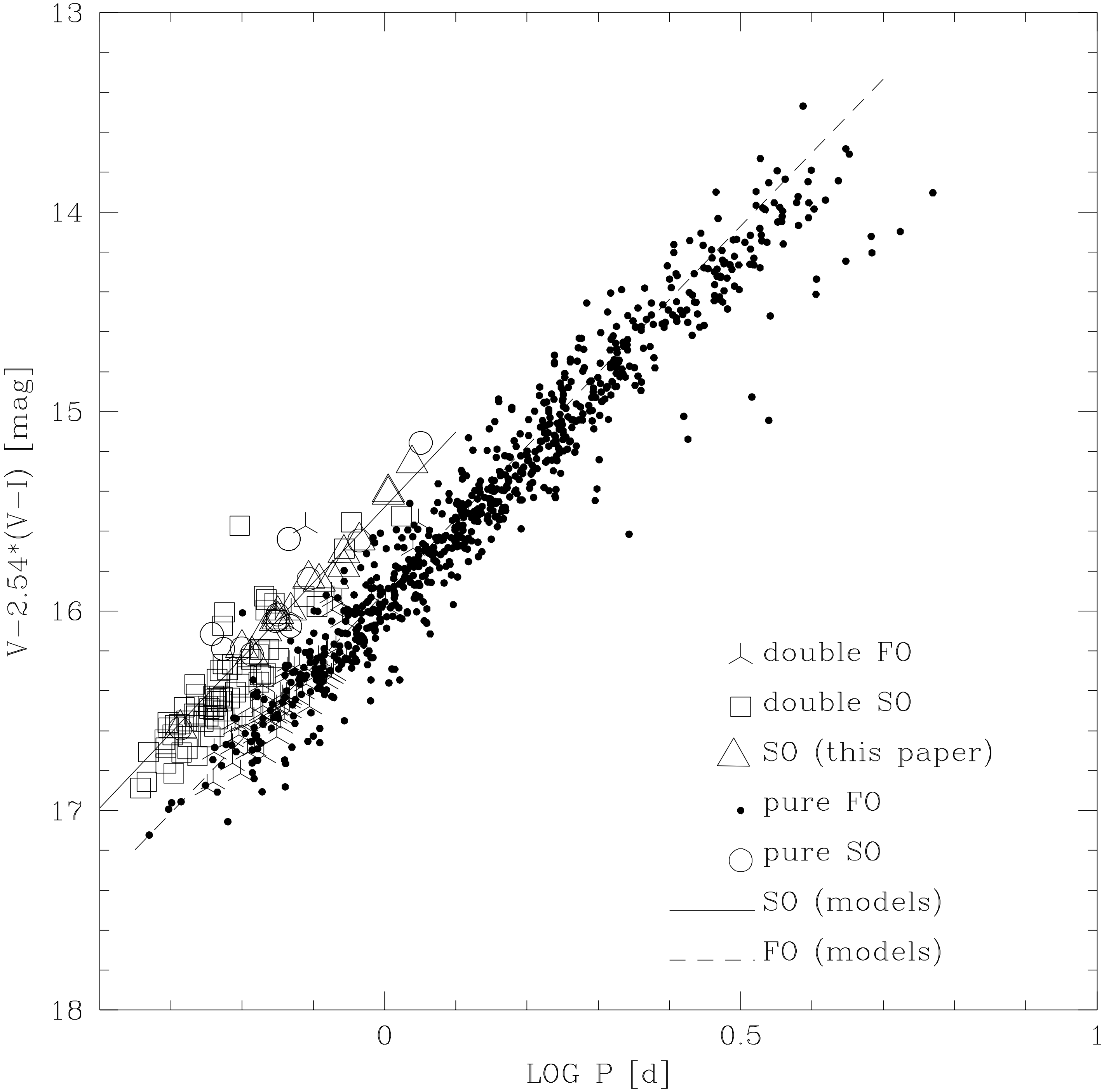
13
14
15
16
17
18
0
0.5
1
V−2.54*(V−I) [mag]
LOG P [d]
double FO
double SO
SO (this paper)
pure FO
pure SO
SO (models)
FO (models)

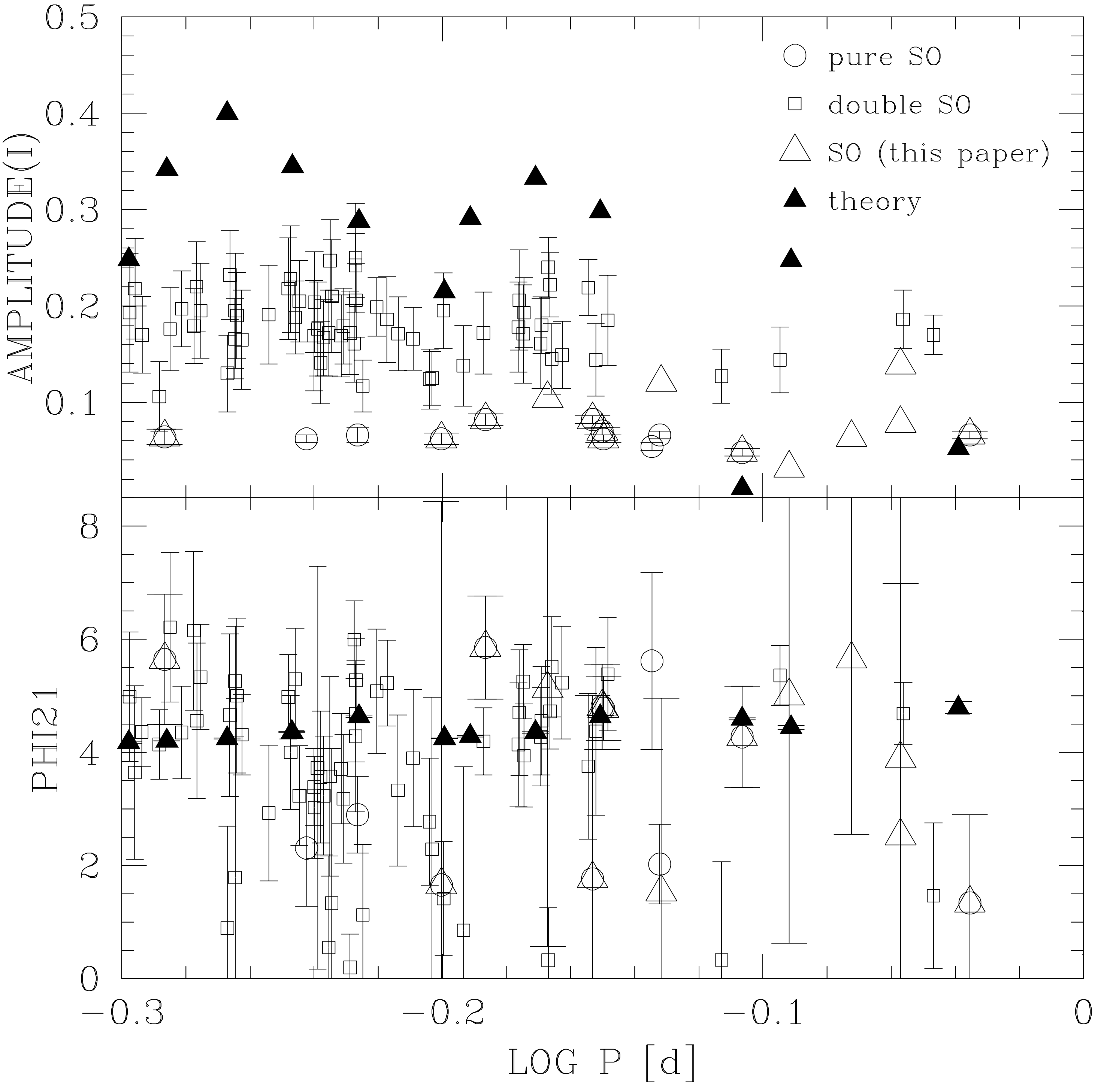

pure S0
double S0
S0 (this paper)
theory
AMPLITUDE(I)
PHI21
LOG P [d]

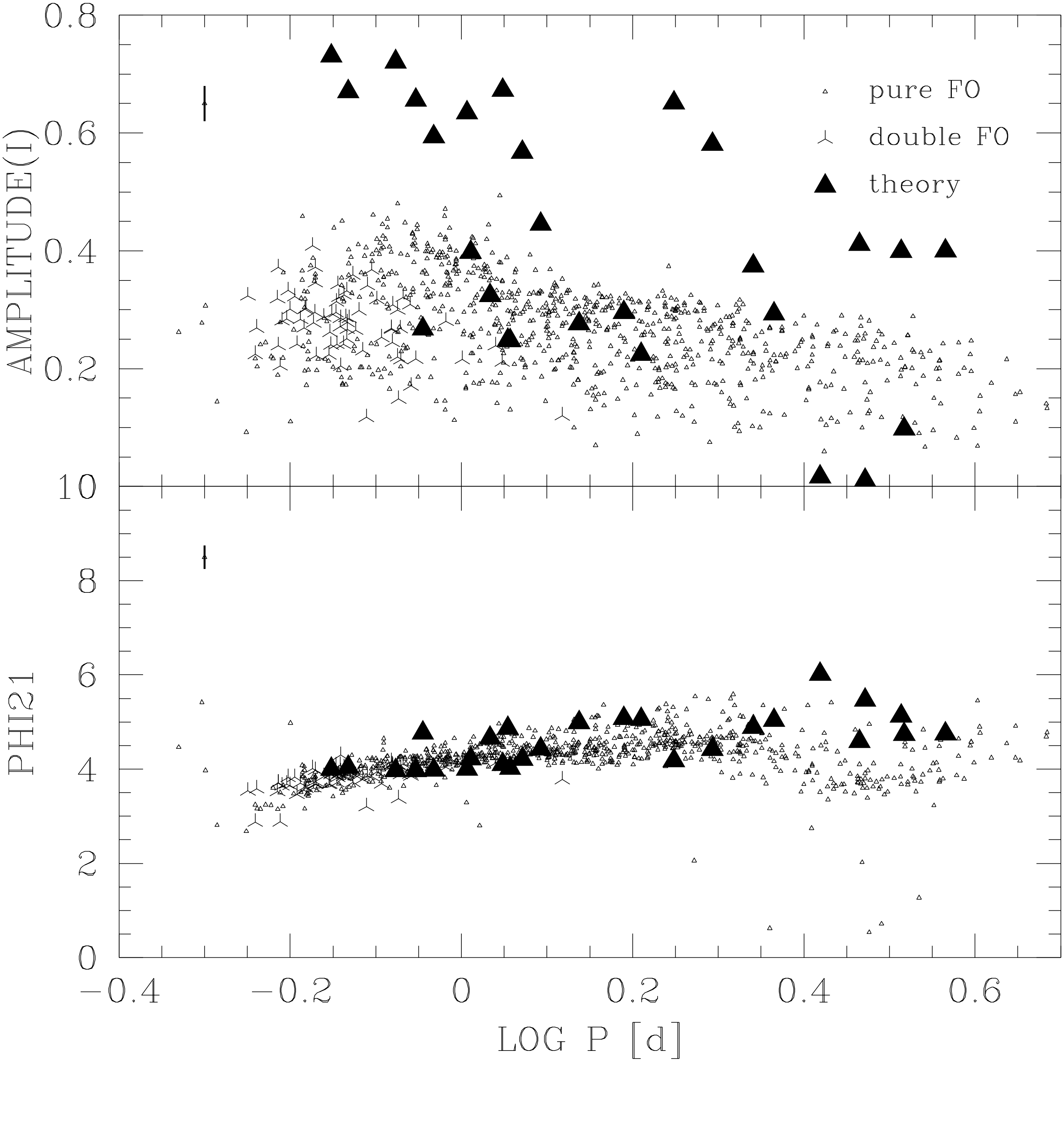

0.8
0.6
0.4
0.2
10
8
6
4
2
0
AMPLITUDE(I)
PHI21
pure FO
double FO
theory
−0.4
−0.2
0
0.2
0.4
0.6
LOG P [d]

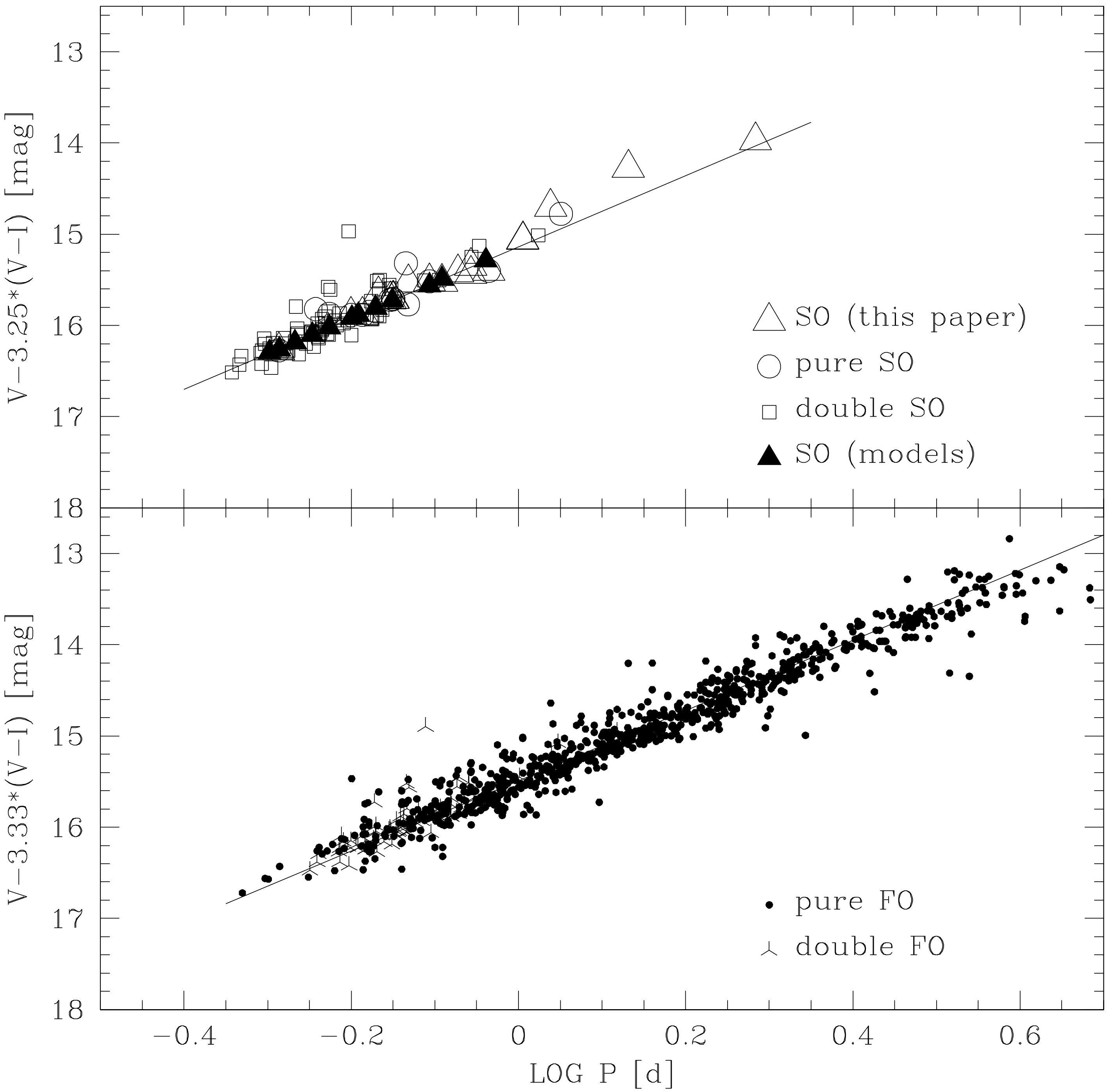

V−3.25*(V−I) [mag]
SO (this paper)
pure SO
double SO
SO (models)
V−3.33*(V−I) [mag]
pure FO
double FO
LOG P [d]